A Two Phase Hybrid RSS/AoA Algorithm for Indoor Device Localization using Visible Light *

Gregary B. Prince and Thomas.D.C. Little
Department of Electrical and Computer Engineering
Boston University, Boston, Massachusetts
{*gbprince, tdcl*}*@bu.edu*

September 19, 2012

MCL Technical Report No. 09-19-2012

Abstract–A two phase hybrid algorithm for estimating the location of a mobile node, which has the capability of measuring signal strength, azimuth, and elevation, in a smart space environment over the visible light channel is proposed. In contrast to conventional triangulation approaches which are performed in a simplified plane, the smart room architecture requires a non-planar solution due to the illumination requirement. Furthermore, conventional triangulation approaches can at times produce numerically ill-defined solutions, thereby prohibiting a notion of target location. Instead of solely relying on triangulation, the mobile nodes estimate their locations through a two phase approach in which they firstly exploit the signal strength observables with unique IDs to establish a *coarse* estimate, and secondly use the azimuth and elevation observables to establish a *fine* estimate. In many cases, the *fine* estimate will improve upon the *coarse* estimate; however when triangulation fails, the algorithm yields the *coarse* estimate rather than a localization failure. Since the environment model relies on the primary requirement of adequate illumination, the number of LED anchors and transmit power for communication functions are determined. Simulation results confirm the effectiveness of the hybrid two phase localization approach in a smart space indoor environment by having a median *coarse* phase accuracy of 34.88 cm and a *fine* phase median accuracy of 13.95 cm.

*In *Proc. IEEE Globecom Conference 2012*, Anaheim, CA Dec 2012. This work is supported by the NSF under grant No. EEC-0812056. Any opinions, findings, and conclusions or recommendations expressed in this material are those of the author(s) and do not necessarily reflect the views of the National Science Foundation.

1 Introduction

Localization has been a subject of growing interest for years as mobile computing is becoming the norm in society. Many of the functions that mobile services provide rely heavily on having some notion of device position. The research field has been flooded with many attempts at balancing performance, cost, and complexity of positioning systems. There have been two main high level approaches set forth to solve the localization problem: (1) exploiting existing infrastructure and developing algorithms to perform the best possible given the infrastructure available and its constraints (e.g. WiFi signal strength, Fluorescent lighting) [4] or (2) designing specialized solutions that address the fundamental issues that are core to the localization problem using the best technologies to solve the problem. Examples of such technologies are Ultrasound, Infrared (IR), Ultrawideband (UWB), [8] and even imaging techniques [9][10][11]. One thought is to use one of the most ubiquitous sources (lighting) in an indoor space to find a balance between infrastructure and technology optimization approaches to indoor localization. Currently, fluorescent lighting using low-rate frequency shift keying waveforms [13][14] and receiver switching methods coupled with a 6-axis sensor for LED lighting [12] have been proposed as solutions in this context. Neither of these approaches take into account the potential for optimally designing the balance between lighting and target localization.

With the introduction of energy efficient LEDs and the world's ever-growing demands for energy, a transition to solid state lighting will happen. LEDs and light for that matter have the ability to offer unparalleled opportunity for mobile computing. Through this infrastructure overhaul researchers have the ability to carefully architect and shape the way light can be used to localize mobile devices but also enable intelligent spaces. Although, the concept of a *smart room* has been gaining attention, it should be noted that localizing and detecting various targets is vital to its operation. Therefore, the task of localization is more complicated as a variety of targets of interest may or may not occupy the space and to date many approaches focus on finding devices that have the ability to communicate, not necessarily people, animals, and even chemicals without incorporating some form of imaging or simple motion sensor.

Section II provides the necessary background description of the Visible Light Communication (VLC) channel and its constraints while touching on the rudimentary localization. Section III describes the system model in which we analyze the lighting and geometric constraints and describe the two phase algorithm. Section IV provides the results in terms of location accuracy for both the coarse and fine phases measured against the ground truth over the constructed indoor environment, while Section V concludes the investigation and proposes areas for new research.

2 Background

Indoor localization has been explored in many contexts, but most often finds application in piggybacking existing communication infrastructures (e.g. WiFi, Bluetooth) due to the fact that customized solutions (e.g. UWB, Ultrasound, and IR) are too expensive and require hardware devoted solely to localization in addition to existing communication infrastructure. Moreover, localization in the conventional sense requires transceivers which are capable of processing channel measurements (e.g. angle, signal strength, time of flight etc.) and relate them to positional estimates through localization algorithms (e.g. multilateration, triangulation). With the transition from elec-

tric to electronic lighting and the ubiquity of light in indoor spaces, visible light may prove to be the next communication infrastructure to exploit for localization services. The benefits of visible light as a localization medium are its directionality, short range, and impulse response, while its issues to overcome are installation accuracy, network layer identification, coexistence of WiFi and VLC [17], and efficient multiple access schemes [5].

To provide a theoretical analysis and simulation of the proposed algorithm, a model of the VLC channel is required. The channel impulse response, $h(t)$, model is that proposed in a characterization of the channel through simulation [2][6] to account for reflections that lead to temporal dispersion in $h(t)$.

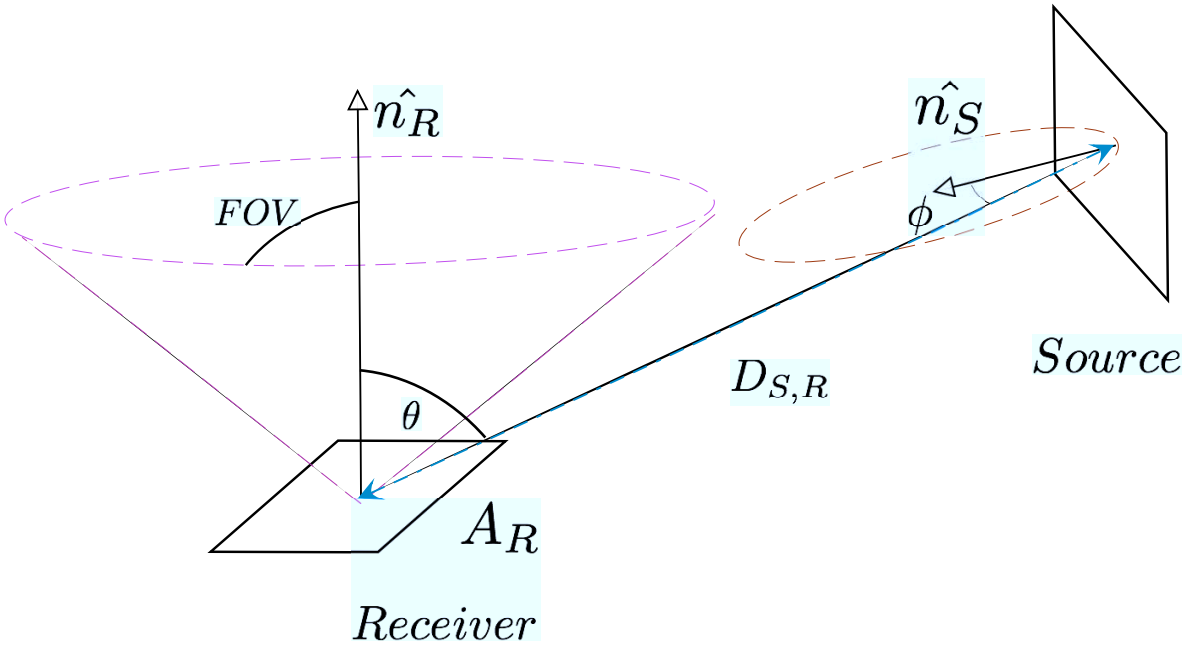

Figure 1: Source Receiver Channel Model Illustration [6]

Due to the directionality of visible light systems, the following vector structure is employed to describe the geometry of a source-receiver pair. A typical LED source can be represented by $\mathcal{S}_k = \{\mathbf{r}_{\mathcal{S}_k}, \hat{\mathbf{n}}_{\mathcal{S}_k}, m_k, P_{T_k}\}$, $\forall k \in L$; $\mathbf{r}_{\mathcal{S}_k} = [x_k, y_k, z_k]^T$ is the source position, $\hat{\mathbf{n}}_{\mathcal{S}_k}$ is the source orientation, m is the Lambertian mode number associated with the directivity of the source, P_{T_k} is the source's transmit power, and L is the number of sources in the space.

Whereas the simple receiver is defined as $\mathcal{R}_j = \{\mathbf{r}_{\mathcal{R}_j}, \hat{\mathbf{n}}_{\mathcal{R}_j}, A_{R_j}, FOV_j\}$, $\forall j \in T$; $\mathbf{r}_{\mathcal{R}_j} = [x_j, y_j, z_j]^T$ is the receiver position, $\hat{\mathbf{n}}_{\mathcal{R}_j}$ is the orientation, A_{R_j} is the receiver area, FOV_j is the receiver's field of view, and T is the number of receivers in the space . Provided a range $D_{k,j}$ between the k^{th}source and the j^{th} receiver, $\theta_{j,k}$ is the angle of incidence between $\hat{\mathbf{n}}_{\mathcal{R}_j}$ and $(\mathbf{r}_{\mathcal{S}_k} - \mathbf{r}_{\mathcal{R}_j})$ and $\phi_{k,j}$ is the angle of irradiance between $\hat{\mathbf{n}}_{\mathcal{S}_k}$ and $(\mathbf{r}_{\mathcal{R}_j} - \mathbf{r}_{\mathcal{S}_k})$.

$$\cos(\theta_{j,k}) = \hat{\mathbf{n}}_{\mathcal{R}_j} \cdot \frac{\mathbf{r}_{\mathcal{S}_k} - \mathbf{r}_{\mathcal{R}_j}}{D_{k,j}} \tag{1}$$

$$\cos(\phi_{k,j}) = \hat{\mathbf{n}}_{\mathcal{S}_k} \cdot \frac{\mathbf{r}_{\mathcal{R}_j} - \mathbf{r}_{\mathcal{S}_k}}{D_{k,j}} \tag{2}$$

Given the performance parameters of the sources and receivers, we can define the maximum possible received power at $(\phi_k, \theta_j) = (0, 0)$, which provides a bound on the power scale the receiver would observe if directly under a luminaire with a perfectly aligned LOS.

$$P_{k,j}(0,0) = \frac{(m_k+1)A_{R_j}P_{T_k}}{2\pi(z_k - z_j)^2} \tag{3}$$

Typically the impulse response of the channel is modeled as a scaled (based on the geometric properties identified) and shifted impulse. This treatment fails to account for the reflections and scattering that are often encountered by optical transmissions; Researchers often account for the multipath effect through an exponential factor κ applied to the propagation model.

$$P_{k,j}(\phi_{k,j}, \theta_{k,j}) = \frac{P_{k,j}(0,0)\cos^{m+\kappa}(\phi_{k,j})\cos^{M}(\theta_{k,j})}{D_{k,j}^2/(z_k - z_j)^2} \tag{4}$$

The development of a software model, CandLES, designed for the specific purpose of characterizing the lighting and communication performance of VLC is provided in [2]. This model can provide the impulse responses for an arbitrary configuration of transceivers and blockage objects along with the illumination pattern without the need for empirically determining an appropriate multipath parameter κ. Furthermore, the transmission is also corrupted by additive white Gaussian noise (AWGN), whose Power Spectral Density (PSD) is constant, at the receiver due to thermal noise.

The PSD of the LED source also has an impact on the communication performance. The PSD of the transmission at the output of the channel is proportional to the PSD of the transmission $PSD_{X_h}(\lambda) \propto PSD_X(\lambda)$.

This produces a PSD, $PSD_{X_h(t)+N(t)}(\lambda)$, which is observed by the receiver optics. Firstly, this signal is concentrated and filtered by to alter the PSD to $PSD_{X_h(t)C}$ which allows the received energy to be optically focused on the detection device (photodiode), $R_{Pd}(\lambda)$ after being appropriately filtered by $R_{OF}(\lambda)$. The signal and noise terms of the received waveform can be expressed as summations over the wavelengths in the band of interest.

$$P = \sum_{\lambda} A \cdot PSD_{X_hC}(\lambda) \cdot R_{OF}(\lambda) \cdot R_{Pd}(\lambda) \cdot \Delta\lambda \tag{5}$$

$$N = \sum_{\lambda} A \cdot PSD_{NC}(\lambda) \cdot R_{OF}(\lambda) \cdot R_{Pd}(\lambda) \cdot \Delta\lambda \tag{6}$$

The SNR can now be defined as the ratio of signal power to the product of unit electron charge, q, the noise, and the signaling rate, R_b.

$$\text{SNR}_{k,j} = \frac{P_{k,j}^2}{(q \cdot N_{k,j}) \cdot R_b} \tag{7}$$

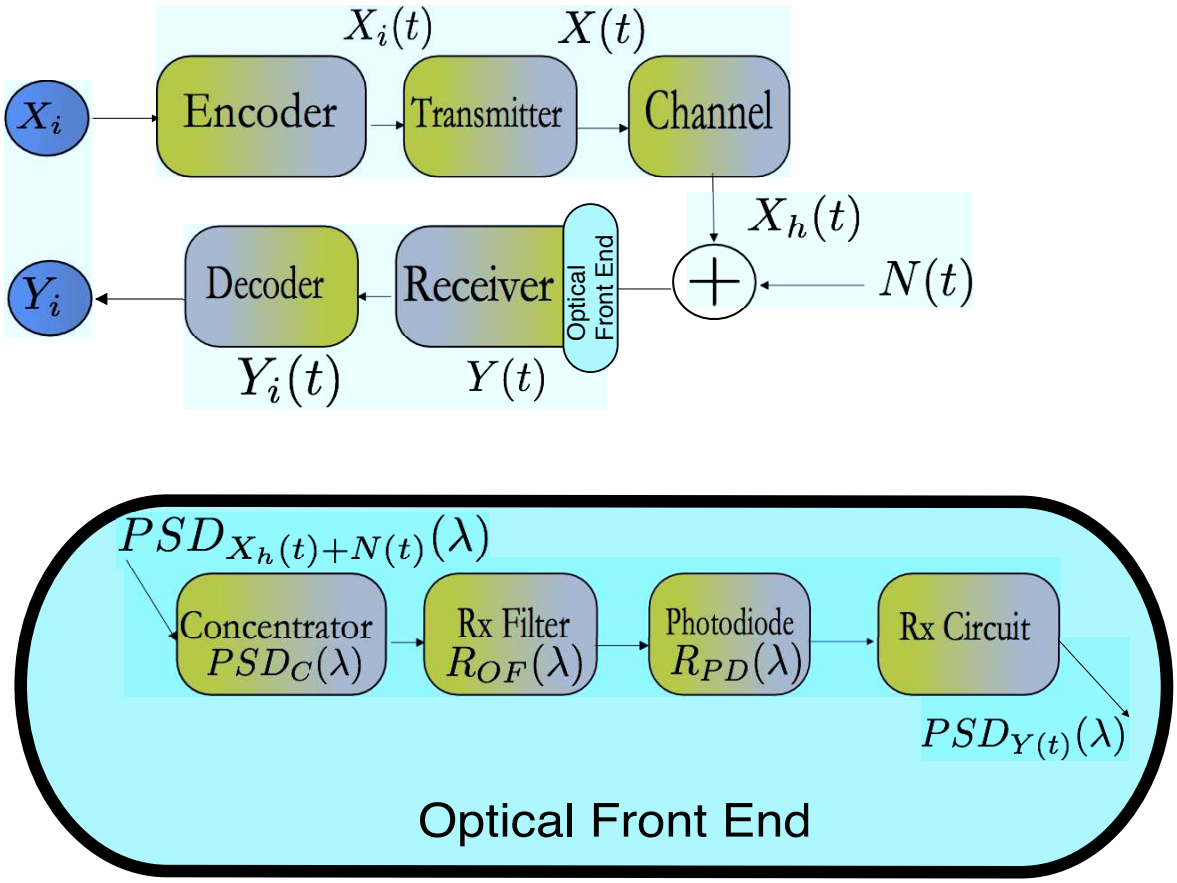

Figure 2: VLC System Blocks: Transmission, Channel, and Reception

With an understanding of the VLC channel, measurements may be extracted from it such as received signal strength (RSS), angle of arrival (AoA), time difference of arrival (TDoA), and/or time of arrival (ToA). Due to the directionality and the short range nature of VLC, some measurement types are more attractive than others when considering localizing a communication capable device. This investigation used RSS and AoA measurements from the visible light channel to determine the target's position.

3 System and Algorithm Description

The CandLES simulation environment [2] is used to model a 4 by 4 by 3.5 meter room, with twelve (12) luminaries mounted to the ceiling and receivers at varying discrete positions within the room. Figure 3 provides a view of the indoor environment model using CandLES. The simulation parameters are provided in Table 1.

The model measures the system impulse response, noise levels, as well as signal power and reception angles at each of the discrete receiver locations from each of the twelve luminaire anchors by coordinating multiple access to the visible light channel in a time division approach. The multiple access scheme may be expanded to use codes, frequency tones, or even wavelengths and

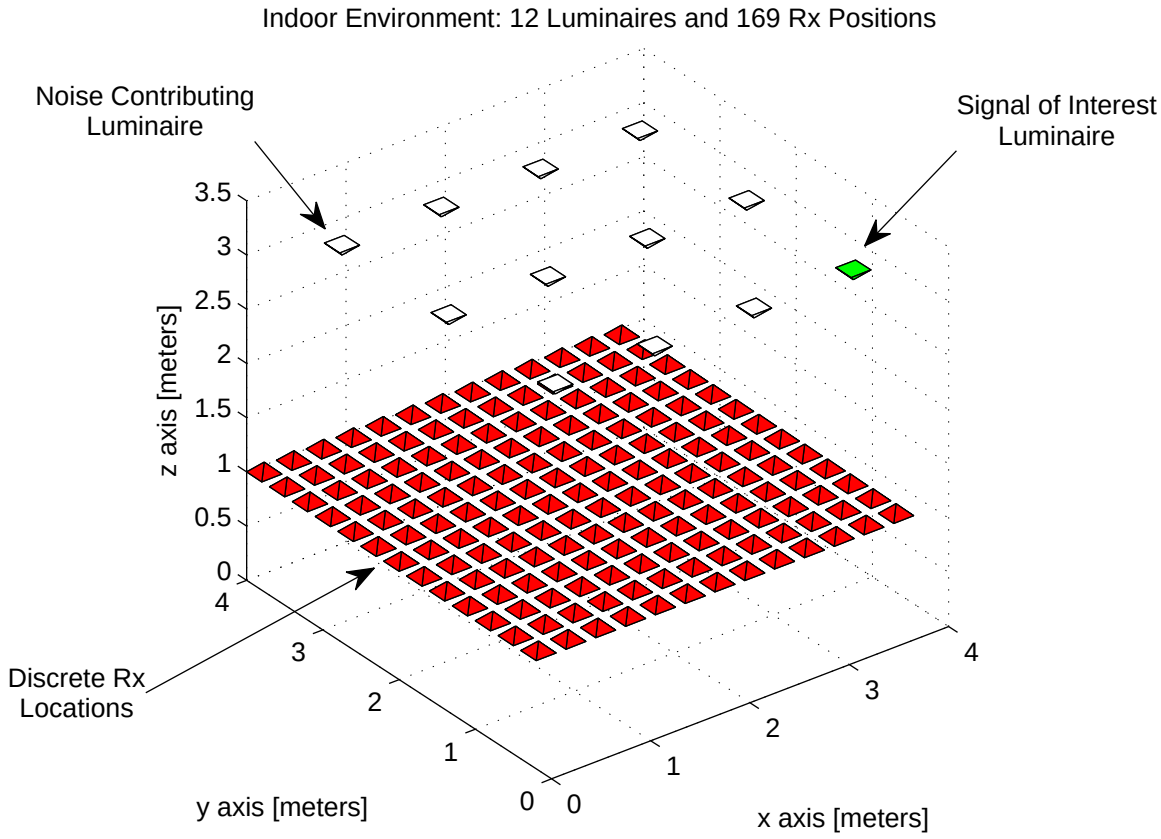

Figure 3: Indoor Environment Model

will be considered in future work. The collection of these measurements within this indoor space are used as input to the proposed localization algorithm herein.

One of the primary requirements of this environment is to provide adequate lighting in the space. As observed in equations (7), the SNR can be very high for adequate illumination. The metric used is 200- 500 lx at desk surface, which is considered to be one meter above the floor. Figure 4 illustrates the illumination coverage in this environment.

3.1 Coarse Phase Algorithm

The *coarse* phase of the target localization algorithm depends heavily on the infrastructure layout of the luminaire anchors. Prior localization approaches in the context of sectors or cells has been investigated [1]. These approaches are able to bound the worst case localization error to the radius of the sector itself through code signaling or in-range sensing.

The context of WiFi/VLC cooperative localization [17] is considered within an indoor environment, equipped with LED luminaries designed and distributed in a manner such that the illumination requirement is satisfied.

The implication of the illumination requirement from a communications perspective, simply guarantees connectivity over the majority of the indoor environment. The k^{th} luminaire is as-

Table 1: Indoor Localization Parameters

Parameter	Value
Optical Tx Power (P_T)	1.9649 W
Lambertian Mode (m)	30
Effective Area of Rx (A_R)	0.81 cm^2
Electron Charge (q)	1.6×10^{-19} C
Background Light Current (I_{bg})	5100 μA
Speed of Light (c)	2.998×10^8 m/s
Noise PSD (N_o)	1.632×10^{-21} W/Hz
Optical/Electrical Efficiency (γ)	0.53
Source Orientation $(\hat{\mathbf{n}}_{\mathcal{S}_k})$	[0,0,-1]^T
Range of Receiver Azimuth Az	0 to π
Range of Receiver Elevation El	0 to π
Receiver Orientation $(\hat{\mathbf{n}}_{\mathcal{R}_j})$	[0,0,0]$^T - [0,0,-1]^T$
Vertical Range $(z_k - z_j)$	2.2 m
Symbol Rate (R_b)	20 MHz
Field of View (FOV)	10-180 degrees
Wall Reflectivity $\%Reflect$	60%

sumed to be installed at a position $\mathbf{r}_{\mathcal{S}_k,\text{desired}}$ in the relative coordinate frame along with its relative orientation $\hat{\mathbf{n}}_{\mathcal{S}_k,\text{desired}}$; however these absolute positions and orientations are subject to installation errors $(\mathbf{r}_{\mathcal{S}_k,\text{offset}}, \hat{\mathbf{n}}_{\mathcal{S}_k,\text{offset}})$, which are modeled as Gaussian noise.

$$\mathbf{r}_{\mathcal{S}_k,\text{actual}} = \mathbf{r}_{\mathcal{S}_k,\text{desired}} + \mathbf{r}_{\mathcal{S}_k,\text{offset}}, \forall k \in L \tag{8}$$

$$\hat{\mathbf{n}}_{\mathcal{S}_k,\text{actual}} = \hat{\mathbf{n}}_{\mathcal{S}_k,\text{desired}} + \hat{\mathbf{n}}_{\mathcal{S}_k,\text{offset}}, \forall k \in L \tag{9}$$

Furthermore, the coarse algorithm leverages the work done on multiple access [5] for the visible light channel. At the network layer each landmark luminaire is required to have its own unique ID, and the capability to packetize the position, orientation, transmit optical power, and beam pattern mode as outlined in the Figure 5. The mobile target has the capability to process the network layer packets and measure the optical power for each luminaire transmission in the sequence and report an estimate when firstly entering the environment. The main idea is that prior to establishing a communication connection, the device broadcasts its presence to the infrastructure. The coarse estimate is obtained as a weighted positional estimate whose weights are the measured optical power from each luminaire. Additional binary weights β_k are applied to the received optical power to discount outliers in the observations, which can occur at varying orientations. This investigation used a received power threshold of 10 dB. Equation 10 outlines the coarse weighted estimate of device location.

$$\hat{\mathbf{r}}_{\mathcal{R}j} = \frac{\sum_{k=1}^{L} \beta_k P_{k,j}(\phi_{k,j}, \theta_{k,j}) \mathbf{r}_{\mathcal{S}_k,\text{desired}}}{\sum_{k=1}^{L} \beta_k P_{k,j}(\phi_{k,j}, \theta_{k,j})} \tag{10}$$

The only constraint on the rate, R_b, at which the coarse sequence is transmitted is that the power level variation appears uniform to the user in the room. Moreover, the specific implementation of

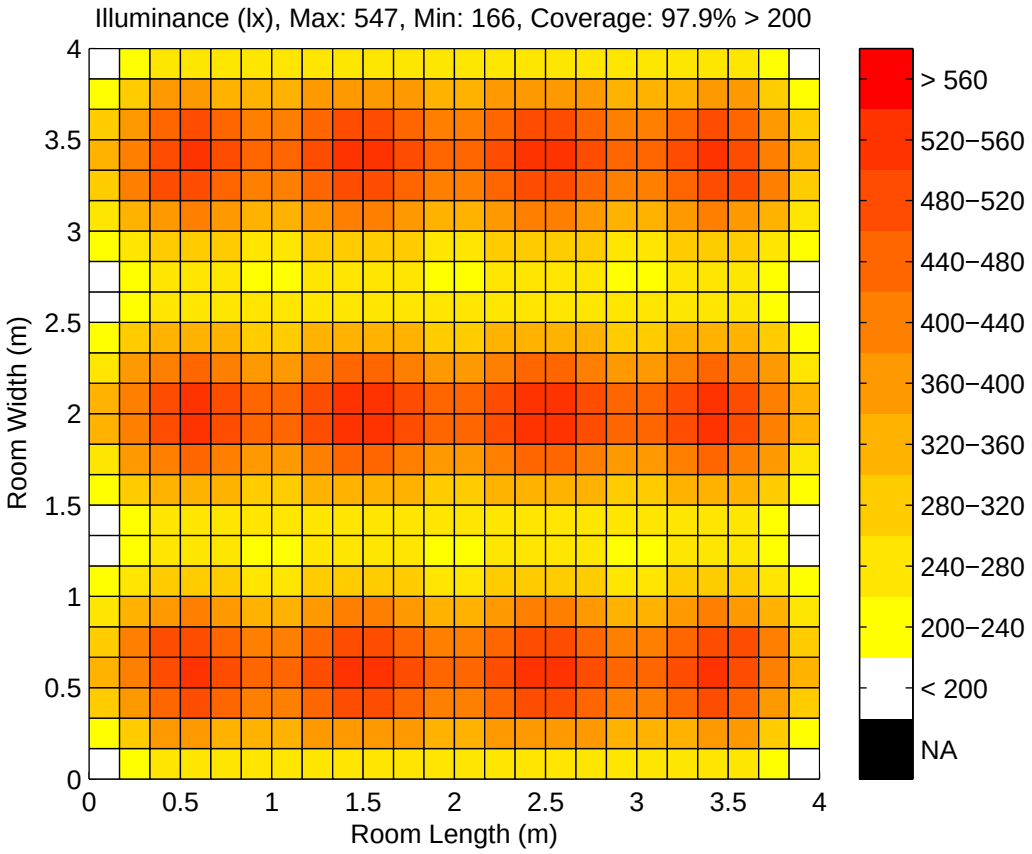

Figure 4: Indoor Environment Illumination Levels at a Height of 1 Meter

AUGMENTATION TO BROADCAST PACKET FOR VLC LANDMARK LUMINAIRES

$SSID_i$	x_i	y_i	z_i	$\hat{n}_{S_i}$	P_T	m

Figure 5: Broadcast VLC Packet

the multiple access is not considered in this paper. One of the largest benefits of this approach is that simply observing the brightest luminaire does not yield an appropriate feasible guess of location, especially when multiple luminaries are within the FoV. The *coarse* phase concludes by returning the AoA measurements it expects to observe in the *fine* phase.

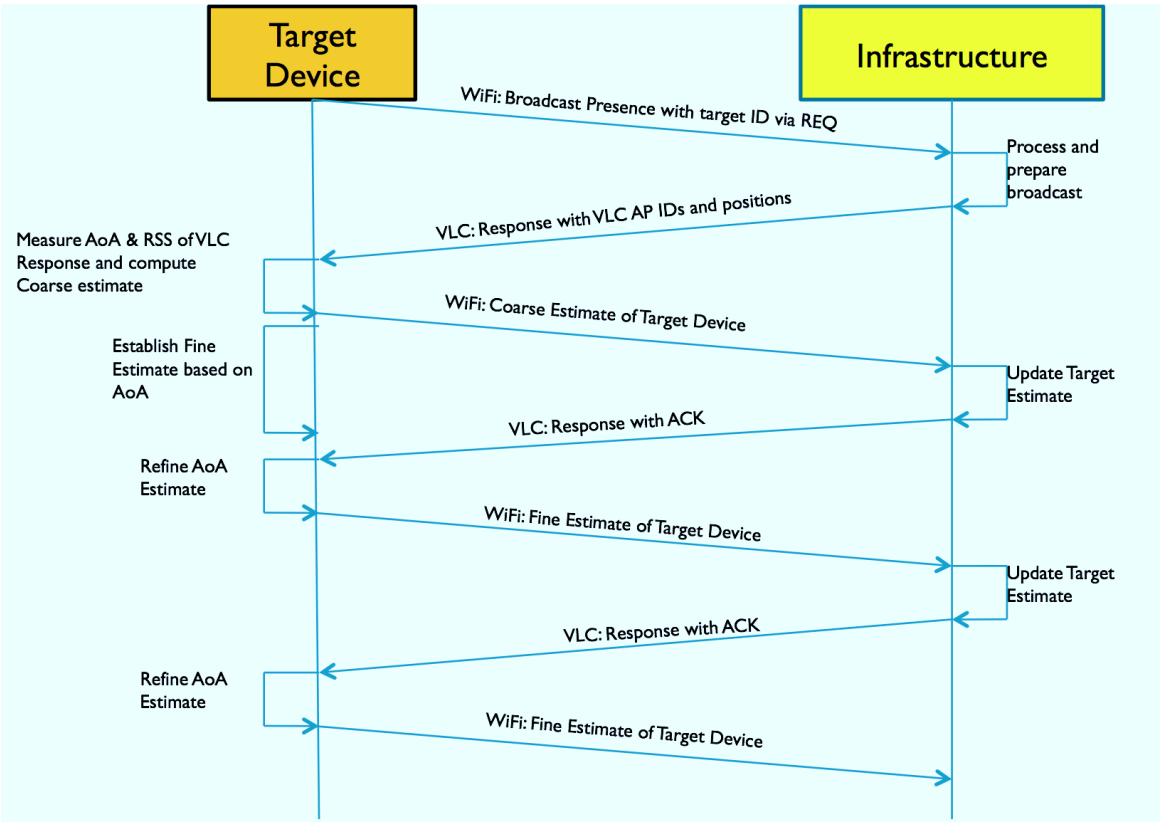

Figure 6: Localization Process between Target and Infrastructure

3.2 Fine Phase Algorithm

The orientation of the target is crucial and the determination of target location is geometry and search related given the information available. The *coarse* phase of the algorithm measured $P_{k,j}(\phi_{k,j}, \theta_{k,j})$ and provided an initial guess of the range, $\hat{D}_{k,j} = ||\hat{\mathbf{r}}_{\mathcal{R}j} - \mathbf{r}_{\mathcal{S}_{k,\text{desired}}}||$. Therefore, In certain circumstances, we may assume that $\theta_{k,j} = \phi_{k,j}, \forall k \in L, j \in M$ Under this assumption, we may compute an estimate for the angle of incidence, $\theta_{k,j}$.

$$\theta_{k,j} = \cos^{-1}\left[\left(\frac{P_{k,j}(\phi_{k,j}, \theta_{k,j})}{P_{k,j}(0,0)}\right)^{\frac{1}{m+M+\kappa}}\right] \tag{11}$$

The *fine* phase of the positioning algorithm served to improve the initial coarse estimate by measuring bearing and elevation angles observed from the landmark luminaries and triangulating its position. There are several approaches to triangulation in the literature such as iterative search,geometric circle intersection, geometric triangulation, Newton-Raphson method [16]. Firstly, to place the AoA analysis discussion into context, give attention to the geometry outlined in Figure 7.

Typically three dimensional triangulation requires four reference anchors due to the fact that each anchor provides one independent AoA measurement to the receiver. However, if the receiver is capable of measuring both Azimuth $(\hat{\psi}_{k,j})$ and Elevation $(\hat{\alpha}_{k,j})$ with respect to its orientation

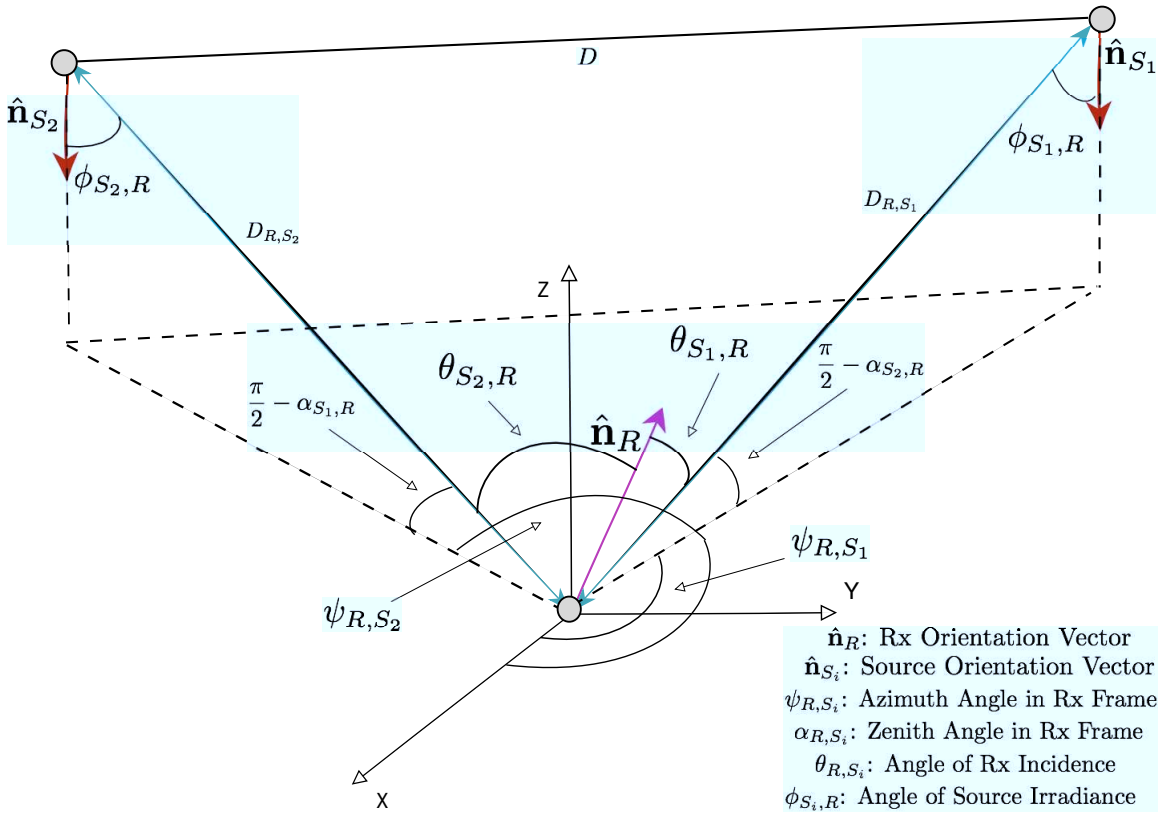

Figure 7: Triangulation Illustration

axis (e.g the z-axis is $\hat{\mathbf{n}}_{\mathcal{R}_j}$) , only two anchors are required for triangulation. Let D_x and D_y denote the inter-luminaire spacing in the x and y directions, mounted on the ceiling. Given these two distances any inter-anchor distance, D, can be computed when determining which anchors to use for triangulation. Furthermore, we may compute the ranges between the anchors $k = 1, 2$ and the j^{th} receiver of interest as follows:

$$D_{j,1} = \frac{D\sqrt{1 + \tan^2 \hat{\psi}_{j,1}}}{\sin \hat{\alpha}_{j,1}(\tan \hat{\psi}_{j,1} \tan \hat{\psi}_{j,2})} \tag{12}$$

$$D_{j,2} = \frac{D\sqrt{1 + \tan^2 \hat{\psi}_{j,2}}}{\sin \hat{\alpha}_{j,2}(\tan \hat{\psi}_{j,1} \tan \hat{\psi}_{j,2})} \tag{13}$$

$$\begin{bmatrix} X_j \\ Y_j \\ Z_j \end{bmatrix} = \begin{bmatrix} X_k \\ Y_k \\ Z_k \end{bmatrix} + \begin{bmatrix} D_{j,k} \sin \hat{\alpha}_{j,k} \cos \hat{\psi}_{j,k} \\ D_{j,k} \sin \hat{\alpha}_{j,k} \sin \hat{\psi}_{j,k} \\ D_{j,k} \cos \hat{\alpha}_{j,k} \end{bmatrix} \tag{14}$$

It can be seen in equations 12 through 14, that given true measurements of the Azimuth ($\hat{\psi}_{k,j} = \psi_{k,j}$) and Elevation ($\hat{\alpha}_{k,j} = \alpha_{k,j}$) between the receiver and two anchor luminaries, the position of the receiver can be analytically computed. Due to the non-linearity of the transformations, bias and precision errors in the angular measurements can drastically affect the estimate of receiver

position. There are measures to be taken to bound the affect these instrumentation errors can propagate. Given that lighting sources are typically installed in a fixed location within the indoor space, we may derive a geometric constraint [18] which aids in the removal of poor measurements. In this paper, however, we assume that the light sources are on the ceiling as in Figure 3 and can derive the geometric constraint according to the illustration in Figure 7.

$$\mathbf{e} = \left[e_{\psi_{1,j}}, e_{\alpha_{1,j}}, e_{\psi_{2,j}}, e_{\alpha_{2,j}}\right]^T \tag{15}$$

We propose to minimize the square error $f(\mathbf{e})$ subject to the geometric constraint $c(\mathbf{e})$.

$$\begin{array}{lrcl} \text{argmin}_{\mathbf{e}} & f(\mathbf{e}) & = & \mathbf{e}^T\mathbf{e} \\ \text{subject to} & c(\mathbf{e}) & = & 0 \end{array} \tag{16}$$

We can observe that the constraint based on this configuration is given by:

$$\begin{array}{rc} c(\mathbf{e}) = & \cot(\frac{\pi}{2} - \alpha_{1,j})\sin(\psi_{1,j}) - \\ & \cot(\frac{\pi}{2} - \alpha_{2,j})\sin(\pi - \psi_{2,j}) = 0 \end{array} \tag{17}$$

This constrained optimization problem may be solved Lagrangian functions and may be transformed into a more computationally effective Quadratic Programming (QP) problem [18]. The optimization is iterative and have pre-established performance criteria established such as an error tolerance ($\gamma \geq 0$): $||\mathbf{e}_{i+1} - \mathbf{e}_i|| \leq \gamma$ to prevent demising returns on computation or subject to a maximum iteration constraint : $I_{max} = N$, to prevent excessive computation time.

4 Results

The two phase hybrid localization system is applied to the environment model (Figure 3), using the range of parameters in Table 1.

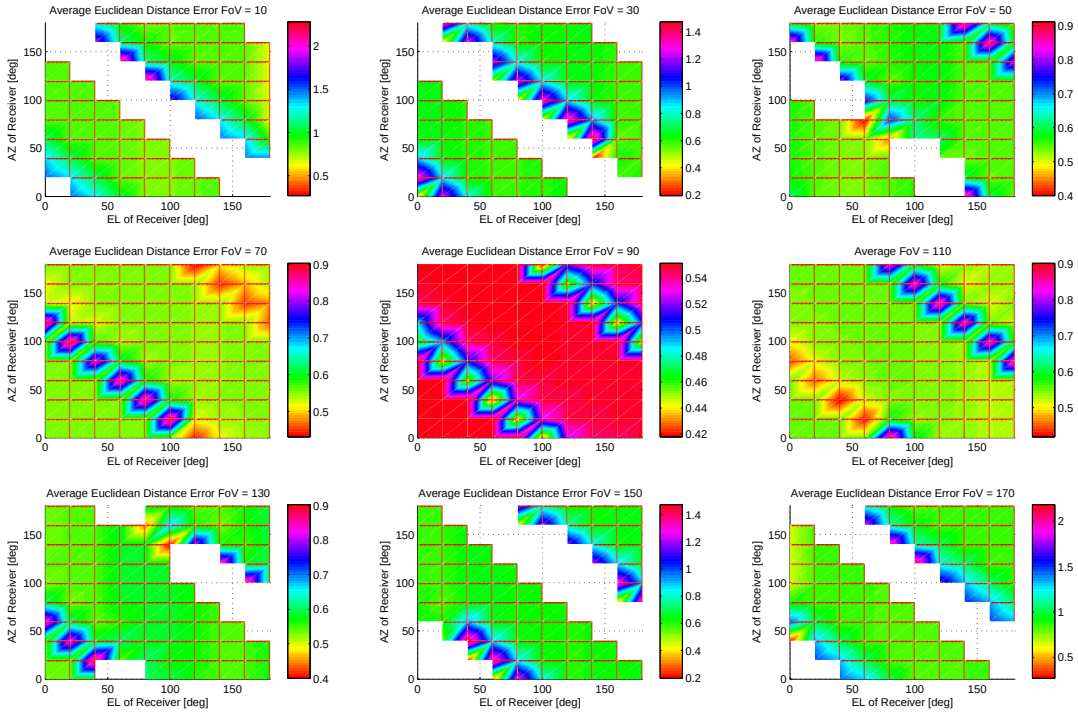

Figure 8: Coarse Performance for Varying Field of Views as a function of Receiver Orientation

Firstly, the effect of orientation and field of view on the receiver design was studied to bound the design space; if the coarse performance is poor or numerically ill defined, the fine phase of the algorithm is of no use. Figure 8 illustrates the mean Euclidean distance error as an intensity plot for fixed field of views as a function of receiver orientation (Azimuth and Elevation in its local coordinate frame).

It is observed that for $FoV \notin [70, 110]$, there are potential orientation configurations in which a coarse estimate cannot be made (as seen as white patches in Figure 8). The 90 degree FoV provides the best mean Euclidean distance accuracy performance over all receiver orientation ranging from **42 cm** to **55 cm** when not being directly beneath luminaries. Taking this result into account, the spatial error distribution is investigated for the coarse phase of the algorithm. The mean accuracy error over the indoor simulation space is found to be **34.88 cm**. The intensity map of accuracy error is shown in Figure 9. The largest spatial contributors of error are the poorly illuminated areas; however occupants are generally not isolated to these corner areas. We can observe that the coarse phase effectively groups the receiver to the closest luminaries or combination thereof, therefore the performance of this scheme is best when the receiver is in the closest proximity to luminaries.

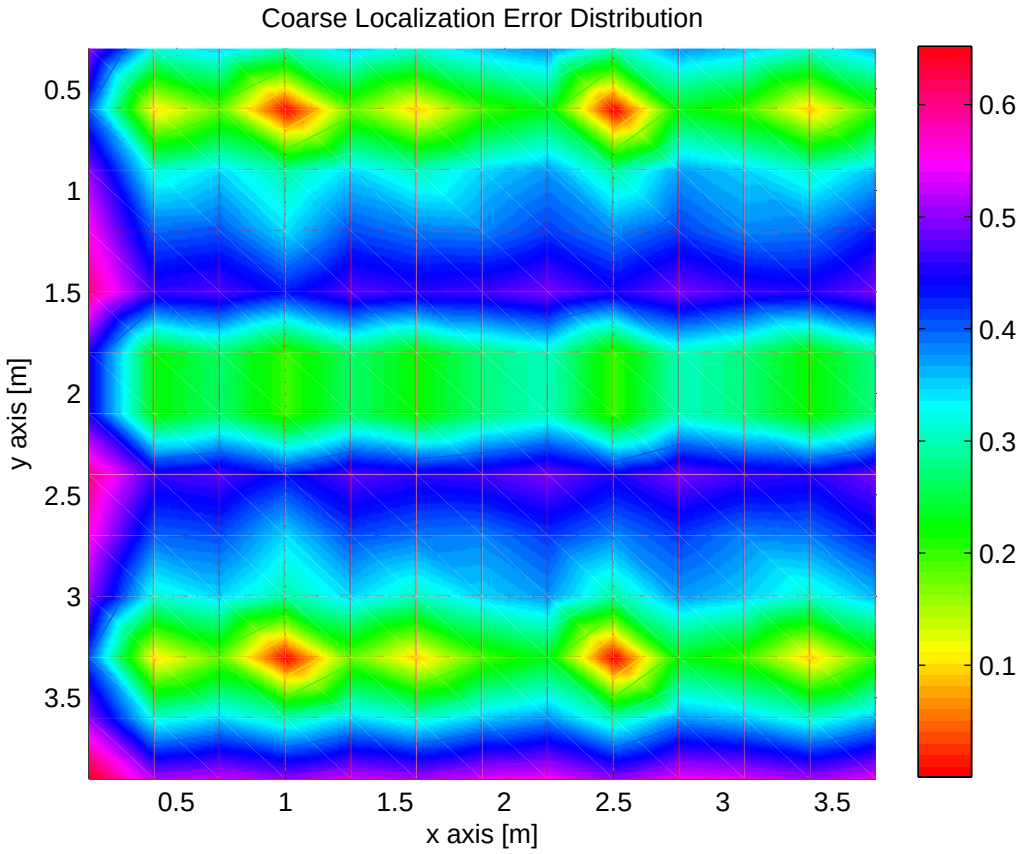

Figure 9: Coarse Algorithm Location Estimation Error Spatial Distribution

The fine phase of the algorithm serves to improve the initial coarse estimate. As observed in Figure 10, the Euclidean distance error is improved over the interior of the room when compared to the coarse phase performance as the receiver is able to arrive at useful independent measurements and can refine the initial coarse estimate. . It is noticed, however, that the fine phase processing has little impact on the poorly illuminated sections of the room. The median accuracy over the complete room is **13.95 cm**.

The results reported offer significant improvements over state of the art piggyback approaches due to both the ubiquity and distribution of anchor sources provided throughout the indoor environment as well as the directionality of the medium over which the localization is performed. Moreover the computational complexity is low as a coarse estimate is found within one multiple access cycle, whereas the fine estimate arrives at a solution within four iterations on average. This algorithm is performed in the mobile device and can be thought of as distributed; however as we have shown herein the device may report its estimates of its location to the infrastructure to allow the infrastructure to provide services or resources to the mobile device.

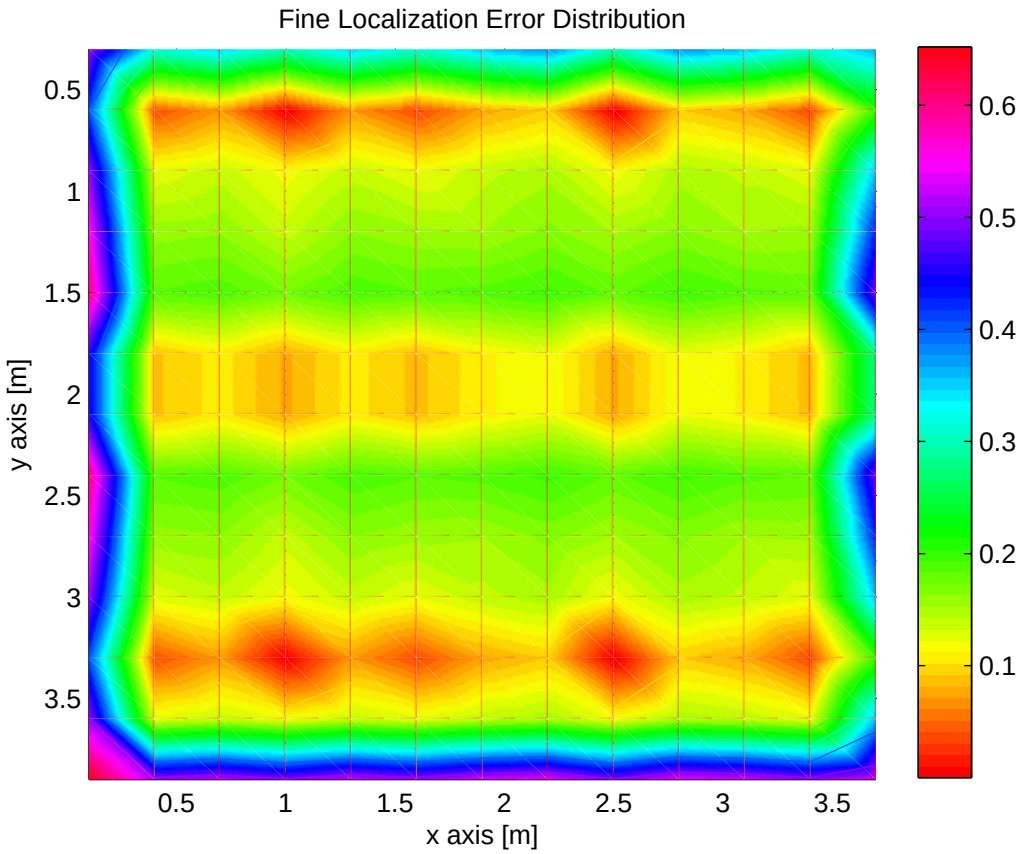

Figure 10: Fine Algorithm Location Estimation Error Spatial Distribution

5 Conclusions and Future Work

Localization algorithms, which adhere to the exploitation of communication infrastructure (e.g. WiFi, Bluetooth), typically perform poorly (e.g. accuracies of 1 meter or more) and moreover often require sophisticated learning algorithms or fingerprinting methods to achieve that performance. A lighting infrastructure based on solid state LED illumination and communication was introduced. It was found that the directionality and increased number of landmarks enabled superior performance using the proposed two phase algorithm than the state of the art approaches for WiFi or Bluetooth. Despite the findings being intuitive from a heuristics standpoint it's the application to lighting (a common indoor necessity) that enables these improvements using simple weighted average and triangulation approaches. Our results show that visible light is one of the most viable solutions to indoor positioning due to its directionality, short impulse response, and the distribution and ubiquity of anchor luminaries to meet the illumination needs of indoor spaces. Future work will consider occupied spaces with more multipath effects are observed along with varying lighting configurations.

References

[1] J. Shen and Y. Oda. Direction Estimation for Cellular Enhanced Cell-ID Positioning using Multiple Sector Observations. *International Conference of Indoor Positioning and Indoor Navigation (IPIN).*, Zürich, Switzerland, September 2010.

[2] M.B. Rahaim, T. Borogovac, and J.B. Carruthers. CandLES - Communication and Lighting Emulation Software. *Proceedings of the 5th ACM international workshop on Wireless netwrok testbeds, experimental evaluation and characterization*, Chicago IL, Septemeber 2010.

[3] F.R. Gfeller and U.H Bapst. Wireless in-House Data Communication via Diffuse Infrared Radiation. *Proceedings of the IEEE*, vol. 67, pp. 1474-1486, November 1979.

[4] E. Elnahrawy, X. Li, and R. P. Martin. The Limits of Localization using Signal Strength: A Comparative Study. *1st IEEE International Conference on Sensor and Ad hoc Communications and Networks (SECON)*, Santa Clara, CA, pp. 406-414, October 2004.

[5] Z. Wu. Free Space Optical Networking with Visible Light: A Multi-hop Multi-access Solution. *Boston University Dissertation*. Dec 2011.

[6] J. R. Barry, J. M. Kahn, W. J. Krause, E. A. Lee, and D. G. Messerschmitt. Simulation of Multipath Impulse Response for Indoor Wireless Optical Channels. *IEEE Journal on Selected Areas in Communications*, vol. 11, pp. 367-379, Apr. 1993.

[7] T. Komine and M. Nakagawa, Fundamental Analysis for Visible-Light Communication System using LED Lights. *IEEE Transactions on Consumer Electron*, vol. 50, no. 1, pp. 100-107, Feb. 2004.

[8] H. Liu, H. Darabi, P. Banerjee, and J. Liu. Survey of Wireless Indoor Positioning Techniques. *IEEE Transaction on Systems, Man, and Cybernetics - Part C: Applications and Reviews*, vol. 37, No. 6, pp. 1067-1080, November 2007.

[9] M. Yoshino, S. Haruyama, and M, Nakagawa. High Accuracy Positioning System using Visible LED Lights and Image Sensor. *IEEE Radio and Wireless Symposium*,pp. 439-442, January 2008.

[10] T. Tanaka and S. Haruyama. New Position Detection Method using Image Sensor and Visible Light LEDs. *Second International Conference on Machine Vision (ICMV)*, pp. 150-153, December 2009.

[11] H. Uchiyama, M. Yoshino, H. Saito, M. Nakagawa, S. Haruyama, T. Kakehashi, and N. Nagamoto. Photogrammetric System using Visible Light Communication . *34th Annual Conference of IEEE Industrial Electronics*, vol. N, pp. 1771-1776, November 2008.

[12] C.Sertthin, E. Tsuji, S. Kuwano, and K.Watanabe . A Switching Estimated Receiver Position Scheme for Visible Light Based Indoor Positioning System. *4th International Symposium on Wireless Pervasive Computing (ISWPC)*, pp. 1 - 5, February 2009.

[13] X. Liu, H. Makino, and K. Mase . Improved Indoor Location Estimation using Fluorescent Light Communication System with a Nine-Channel Receiver. *IEICE Transactions of Communications*, vol. E93-B, No.11, pp. 2936-2944, November 2010.

[14] X. Liu, H. Makino, S. Kobayashi, and Y.Maeda . Research of Practical Indoor Guidance Platform using Fluorescent Light Communication. *IEICE Transactions of Communications*, vol. E91-B, No.11, pp. 3507-3515, November 2008.

[15] J. Chen and A.Abedi . A Hybrid Framework for Radio Localization in Broadband Wireless Systems. *IEEE Global Communications Conference*, pp. 1 - 6, December 2010.

[16] C. Cohen and F.Koss . A Comprehensive Study of Three Object Triangulation. *Mobile Robots VII*, Vol. 1831, No. 1. pp. 95-106, 1993.

[17] M. Rahaim, A.M. Vegni, and T.D.C. Little. A Hybrid Radio Frequency and Broadcast Visible Light Communication System *Proc. IEEE Globecom 2011 2nd Workshop on Optical Wireless Communications* (OWC 2011), pp. 818-822, Dec. 5-9, 2011, Houston, TX, USA.

[18] A. N. Bishop, B. D. O. Anderson, B. Fidan, P. N. Pathirana, Guoqiang Mao. Bearing-Only Localization using Geometrically Constrained Optimization *Aerospace and Electronic Systems, IEEE Transactions on In Aerospace and Electronic Systems, IEEE Transactions on*, Vol. 45, No. 1. (27 March 2009), pp. 308-320.